A Fluorescence Energy Transfer Method for Analyzing Protein Oligomeric Structure: Application to Phospholamban

Ming Li,* Laxma G. Reddy,* Roberta Bennett,* Norberto D. Silva, Jr#, Larry R. Jones§, and David D. Thomas*
*Department of Biochemistry, University of Minnesota Medical School, Minneapolis, Minnesota 55455; #Mayo Clinic, Guggenheim 14, 200 First St. SW, Rochester, Minnesota 55905; §Krannert Institute of Cardiology, Indiana University, Indianapolis, Indiana 46202

ABSTRACT We have developed a method using fluorescence energy transfer (FET) to analyze protein oligomeric structure. Two populations of a protein are labeled with fluorescent donor and acceptor, respectively, then mixed at a defined donor/acceptor ratio. A theoretical simulation, assuming random mixing and association among protein subunits in a ring-shaped homo-oligomer, was used to determine the dependence of FET on the number of subunits, the distance between labeled sites on different subunits, and the fraction of subunits remaining monomeric. By measuring FET as a function of the donor/acceptor ratio, the above parameters of the oligomeric structure can be resolved over a substantial range of their values. We used this approach to investigate the oligomeric structure of phospholamban (PLB), a 52-amino acid protein in cardiac sarcoplasmic reticulum (SR). Phosphorylation of PLB regulates the SR Ca-ATPase. Because PLB exists primarily as a homopentamer on sodium dodecyl sulfate polyacrylamide gel electrophoresis, it has been proposed that the pentameric structure of PLB is important for its regulatory function. However, this hypothesis must be tested by determining directly the oligomeric structure of PLB in the lipid membrane. To accomplish this goal, PLB was labeled at Lys-3 in the cytoplasmic domain, with two different amine-reactive donor/acceptor pairs, which gave very similar FET results. In detergent solutions, FET was not observed unless the sample was first boiled to facilitate subunit mixing. In lipid bilayers, FET was observed at 25°C without boiling, indicating a dynamic equilibrium among PLB subunits in the membrane. Analysis of the FET data indicated that the dye-labeled PLB is predominantly in oligomers having at least 8 subunits, that 7–23% of the PLB subunits are monomeric, and that the distance between dyes on adjacent PLB subunits is about 10 Å. A point mutation of PLB (L37A) that runs as monomer on SDS-PAGE showed no energy transfer, confirming its monomeric state in the membrane. We conclude that FET is a powerful approach for analyzing the oligomeric structure of PLB, and this method is applicable to other oligomeric proteins.

INTRODUCTION

Protein–protein interactions are crucial for many biological functions, especially in membranes, so quantitative analyses of protein oligomeric structures are needed. Fluorescence energy transfer (FET) has been used to measure self-association of membrane proteins, because FET between subunits usually requires proximity on the order of 6 nm or less, which usually requires protein self-association (Vanderkooi et al., 1977). Since then, quantitative measurement of oligomeric state of proteins using FET has been developed by many investigators (e.g., Veatch and Stryer, 1977; Moens et al., 1994; Adair and Engelman, 1994). However, because of the complexity of the results, the number of subunits considered in these analyses has typically been less than 5, and the approximations made have limited the amount of information obtained about the size and structure of the oligomeric complex. In the present study, we have derived a general expression for FET within a ring-structured oligomer, and have simulated the predicted results numerically. The results show that the energy transfer efficiency is sensitive to the number of subunits within the oligomer, the fraction of protein present as monomers, and the distance between subunits in the oligomer.

To demonstrate the utility of this method, we used it to analyze the oligomeric structure of phospholamban (PLB), a 52-amino acid protein in cardiac sarcoplasmic reticulum (SR). The activity of the cardiac calcium pump (Ca-ATPase) is modulated by PLB, through a phosphorylation-dependent regulation mechanism. In its unphosphorylated state, PLB inhibits the Ca-ATPase at submicromolar calcium concentrations, but the inhibition is relieved upon PLB phosphorylation. This regulation of Ca-ATPase through PLB phosphorylation is proposed to be the underlying mechanism for β-adrenergic stimulation of the heart (Lindemann et al., 1983; Wegener et al., 1989; Luo et al., 1994; Simmerman and Jones, 1998). Both sodium dodecyl

Received for publication 13 July 1998 and in final form 19 February 1999.

Address reprint requests to David D. Thomas, Department of Biochemistry, University of Minnesota Medical School, Minneapolis, MN 55455.

This work was supported by grants to DDT from the National Institutes of Health (GM27906, AR32961) and the Minnesota Supercomputer Institutes. LRJ was supported by grants (HL06308 and HL49428) from the National Institutes of Health. LGR was supported by a grant from the American Heart Association.

Abbreviations used: FET, fluorescence energy transfer; AMCA-S, 7-amino-3-(((succinimidyl)oxyl)carbonyl)methyl)-4-methylcoumarin-6-sulfonic acid; ATP, adenosine triphosphate; CSU, catalytic subunit of cyclic adenosine monophosphate-dependent protein kinase; DABSYL, 4-dimethylaminoazobenzene-4′-sulfonyl chloride; DABCYL, 4-((4-(dimethylamino)phenyl)azo)benzoic acid succinimidyl ester; DANSCL, 2-dimethylaminonaphthalene-6-sulfonyl chloride; DOPC, dioleoyl phosphotidylcholine; DTT, dithiothreitol; EPR, electron paramagnetic resonance; MOPS, 3-(*N*-morpholino)propanesulfonic acid; OG, octylglucoside; PLB, phospholamban; SDS, sodium dodecyl sulfate; SDS-PAGE, sodium dodecyl sulfate-polyacrylamide gel electrophoresis; SEM, standard error of the mean; SR, sarcoplasmic reticulum.

0006-3495/99/05/2587/13 $2.00

sulfate polyacrylamide gel electrophoresis (SDS-PAGE) (Wegener and Jones, 1984) and low-angle laser light scattering results (Watanabe et al., 1991) showed that PLB is a homopentamer in SDS solution. It has been proposed that the pentameric form of PLB is important for the mechanism of Ca-pump regulation (Kovacs et al., 1988; Colyer, 1993; Kimura et al., 1997; Autry and Jones, 1997). The effects of amino acid substitutions on the stability of PLB pentamer in SDS solution have led to a model for a tightly packed coiled-coil pentamer (Simmerman et al., 1996; Arkin et al., 1994), in which the α-helical transmembrane domains of five monomers associate by intramembrane leucine/isoleucine zipper interactions (Simmerman et al., 1996; Karim et al., 1998; Thomas et al., 1998). A point mutation in the proposed zipper region, in which Leu-37 was changed to Ala (L37A), drastically reduces the ability of PLB to form oligomers; this mutant exhibits mainly monomers on SDS gels (Simmerman et al., 1996). Nevertheless, L37A-PLB has been shown to be even more effective than wild-type PLB when coexpressed with the Ca-pump (Kimura et al., 1997; Autry and Jones, 1997), leading to models in which oligomeric changes in PLB play a role in its inhibitory function (Kimura et al., 1997; Cornea et al., 1997). However, the quaternary structure of PLB in SDS is not necessarily the same as in the native membrane environment. To obtain information more closely related to the oligomeric structure of PLB in its native membrane environment, measurements must be performed in lipid bilayers in the absence of detergent.

The first study to measure the oligomeric state of PLB in lipid bilayers used EPR spectroscopy to show that PLB exists in an average oligomeric size of 3.5 in DOPC bilayers, changing to 5.3 upon phosphorylation (Cornea et al., 1997). This study suggested that a dynamic equilibrium exists between PLB subunits in the lipid bilayer, and that the regulation of PLB's oligomeric state is important for its regulation of the Ca-pump. However, the method used in this study (EPR) only measured the average oligomeric size and could not resolve multiple oligomeric species; second, the method used spin-labeled lipid to measure the total intraoligomeric surface area of protein in the membrane, and thus cannot be used to study PLB's oligomeric state in the presence of the Ca-ATPase.

The FET method, presented in this work, overcomes the above restrictions. It resolves multiple oligomeric species, and can be applied to analyze the oligomeric structure of PLB in a variety of environments (detergents versus lipid; in the presence versus absence of Ca-ATPase). Using this method, we examined the oligomeric structure of PLB in detergent solutions and lipid bilayers, and we investigated the effect of PLB phosphorylation.

METHODS

Reagents

Protein kinase A catalytic subunit (PKA-CSU) purified from porcine heart and adenosine triphosphate (ATP) were purchased from Sigma Chemical Co. (St. Louis, MO). *N*-Octyl-β-D-glucopyranoside (OG), sodium dodecyl sulfate (SDS), and $C_{12}E_8$ were purchased from Cal-Biochem (San Diego, CA). Dioleoyl phosphatidylcholine (DOPC) was purchased from Avanti Polar Lipids (Alabaster, AL). The reagents for SDS-PAGE were purchased from Bio-Rad Laboratories (Richmond, CA). The phosphatase inhibitor, calyculin A, was obtained from LC Laboratories (San Diego, CA). The amino-reactive fluorescent dyes, AMCA-S, DABSYL, DANSCL, and DABCYL were purchased from Molecular Probes (Eugene, OR).

Preparation of PLB

Recombinant PLB was expressed in Sf21 insect cells and purified as previously described (Reddy et al., 1995; Simmerman et al., 1996). PLB concentration was determined by the amido black assay (Schaffner and Weissman, 1973). The purified protein was stored at -70°C at a protein concentration of 1–2 mg/mL, in a buffer containing 18 mM glycine, 88 mM MOPS, 5 mM DTT, and 0.92% octyl glucoside (OG) at pH 7.2 (PLB Buffer). Unless otherwise indicated, all sample preparations and measurements were carried out at 25°C.

Labeling PLB with fluorescent dyes

PLB, 100 μg, in PLB Buffer was washed six times in a centricon-3 tube with the labeling buffer (100 mM $NaHCO_3$, 0.01% $C_{12}E_8$, pH 8.3). The washed PLB sample was adjusted to a protein concentration of 1 mg/mL and incubated with one of the fluorescent dyes (AMCA-S, DABCYL, DANSCL, and DABSYL), added from DMF stock solutions at [dye]/[PLB] = 10, at 25°C overnight. To improve the specificity of dye labeling at Lys-3 (see Results), the sample was treated for 60 min with 10 mM DTT at 25°C (Reddy et al., 1999). The incubation was then washed eight times in a Centricon-3 tube, with 20 mM MOPS, 5 mM $MgCl_2$, 0.01% $C_{12}E_8$, pH 7.0 to remove the unreacted free dye. The dye concentration was measured by absorbance, using extinction coefficients of ϵ(345 nm) = 22,000 M^{-1} cm^{-1} for AMCA conjugates, ϵ(443 nm) = 37,000 for DABC conjugates (measured with AMCA- and DABC-*N*-acetyl-Lys-amide), ϵ(326 nm) = 5700 M^{-1} cm^{-1}, and ϵ(472 nm) = 22,000 M^{-1} cm^{-1} for DANS and DABS conjugates, respectively (Adair and Engelman, 1994). The PLB concentration was measured by the amido black assay (Schaffner and Weissman, 1973), which was unaffected by bound dyes.

Reconstitution of PLB into lipid bilayers

Lipid bilayers containing PLB were prepared essentially as described previously (Cornea et al., 1997; Li et al., 1998), except that $C_{12}E_8$ was used instead of OG: A solution containing 5 μM dye-labeled PLB in 0.01% $C_{12}E_8$, 100 mM KCl, 20 mM MOPS, pH 7.0, was added to a dried film of DOPC, usually at a ratio of 100 mol lipid per mol PLB. The mixture was incubated for 1 h with frequent vortexing. Then 200 μL of 20 mM MOPS, 100 mM KCl, pH 7.0 (reconstitution buffer) was added to the mixture, and the sample was subjected to 15 min incubation with vortexing and 5 min in a bath sonicator. The sample was then diluted with another 0.8 mL of reconstitution buffer and centrifuged in a Beckman TL-100 centrifuge at 100,000 rpm for 2 h. The pellet was resuspended in 100 μL of 20 mM MOPS, 5 mM $MgCl_2$, pH 7.0 (DOPC Buffer) and sonicated for 1 min.

Phosphorylation of PLB

For phosphorylation, 6 μg dye-labeled PLB was incubated at 30°C for 12 h in 92 μL of a buffer containing 20 mM MOPS, 5 mM $MgCl_2$, 0.9% OG, and 130 IU/mL of PKA-CSU, pH 7.0 (phosphorylation buffer). The phosphorylation reaction was initiated by adding ATP to a final concentration of 0.6 mM. ATP was omitted from the control (unphosphorylated) sample. The reaction was stopped with concentrated SDS-PAGE running buffer. To phosphorylate lipid-reconstituted PLB, we used the same procedure except that OG was excluded from the phosphorylation buffer. To ensure the

access of CSU and ATP to occluded PLB, we included three freeze/thaw steps after the addition of ATP. These samples were then subjected to electrophoresis and fluorescence measurements. The extent of PLB phosphorylation was quantitated by SDS-PAGE and immunoblot as the fraction of the PLB pentamer band that shifted to decreased mobility (Li et al., 1998).

Fluorescence spectroscopy

Fluorescence was measured in a 3 × 3 mm quartz cuvette. Emission spectra were recorded using an SPEX-Fluorolog II spectrofluorometer (Edison, NJ), with excitation at 330 nm. Both excitation and emission bandwidths were set at 7 nm. Light scattering had no significant effect on the spectrum, as verified by scanning the emission near the excitation wavelength. Each emission spectrum was the average of 4 scans (from 350 nm to 550 nm) with a step size of 1 nm and an integration time of 0.5 s/step. Each fluorescence spectrum was corrected by subtracting a corresponding buffer blank lacking PLB, and the intensity was corrected for the sensitivity of the detector, using a standard lamp. Total fluorescence was measured by integrating the spectrum.

For time-resolved fluorescence measurement, we used a time-correlated single-photon counting system. The light source was a pyridine dye laser pumped by a mode-locked, frequency-doubled YAG laser. The emission was measured with a Hamamatsu multichannel plate photomultiplier tube. Lifetimes τ were determined by least-squares fits to

$$\frac{F(t)}{F(0)} = \sum_{i=1}^{n} a_i \exp(-t/\tau_i). \quad (1)$$

The mean lifetime $\langle\tau\rangle$ is defined as

$$\langle\tau\rangle = \sum_{i=1}^{n} a_i\tau_i \Big/ \left(\sum a_i\right). \quad (2)$$

Fluorescence energy transfer

Two samples of PLB were labeled separately with either fluorescent donor or acceptor, then mixed at a defined donor/acceptor ratio in detergent (usually 0.01% $C_{12}E_8$). For FET in detergents, the mixed samples were heated to 100°C for 5 min, then cooled to 25°C for at least 20 min before fluorescence measurement. For FET in lipid, the mixed samples were reconstituted into DOPC bilayers as described above. Steady-state fluorescence energy transfer was measured from the decrease in donor fluorescence intensity caused by the presence of the acceptor,

$$E = 1 - (F_{DA}/F_D), \quad (3)$$

where E is the FET efficiency, F_{DA} is the donor fluorescence with acceptor present (normalized by donor concentration), and F_D is the donor fluorescence without acceptor present.

Time-resolved FET was measured from the decrease in the excited-state lifetime (τ) of the donor caused by the acceptor

$$E = 1 - (\tau_{DA}/\tau_D). \quad (4)$$

Analysis of E in terms of oligomeric structure (discussed below) requires calculation of the Förster distance R_0, which was calculated from

$$R_0 = 9790(J\kappa^2 n^{-4}\phi_d)^{1/6}, \quad (5)$$

where the orientation factor κ^2 is assumed to be ⅔, corresponding to random orientation; the refractive index of the medium n is assumed to be 1.33 in water; and the spectral overlap integral J is calculated according to

$$J = \int f(\lambda)\epsilon(\lambda)\lambda^4 \, d\lambda, \quad (6)$$

which was calculated from the emission spectrum of the donor, $f(\lambda)$, and the absorption spectrum of the acceptor, $\epsilon(\lambda)$, (Fig. 1) using a computer program written by J. Mersol. The quantum yield ϕ_d for the DANS conjugate was assumed to be 0.36 (Chen, 1966); and that for the AMCA conjugate was measured to be 0.48 for AMCA-*N*-acetyl-Lys-amide, using DANS-*N*-acetyl-Lys-amide as a standard [ϕ_d = 0.36 (Chen, 1966)].

RESULTS

Calculation of FET in oligomers

In an oligomeric complex with n subunits, with all subunits labeled with either donor or acceptor and mixed randomly, the energy transfer efficiency (E), computed in terms of the binomial distribution of the number of donors in an oligomer, is

$$E = 1 - 1/[n(1 - P_a)]\sum_{i=1}^{n} i*\binom{n}{i} * P_a^{n-i} * (1 - P_a)^i * [1 - E_i(R)], \quad (7)$$

where n is the number of subunits in the oligomer, P_a is the mole fraction of acceptor, and $(1 - P_a)$ is the mole fraction of the donor. Variable R is the distance between donor and acceptor pairs on different subunits, and $E_i(R)$ is the averaged transfer efficiency when there are i donors in the oligomer. The other factors in each term of the summation give the probability of having i donors in an oligomer.

As n increases, it becomes difficult to write out all the combinations in the expression for $E_i(R)$. In previous studies, approximations have been made, assuming either equal energy transfer to all subunits (Veatch and Stryer, 1977; Adair and Engelman, 1994) or zero energy transfer to dis-

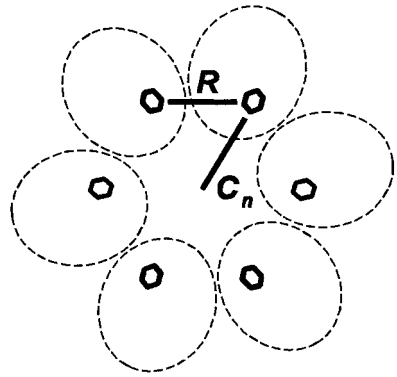

FIGURE 1 Symmetrically assembled, circular ring oligomer (shown here as a hexamer, n = 6), as assumed for FET simulations. R, distance between dyes labeled on neighboring subunits. C_n, radius of the ring as measured to the center of each dye.

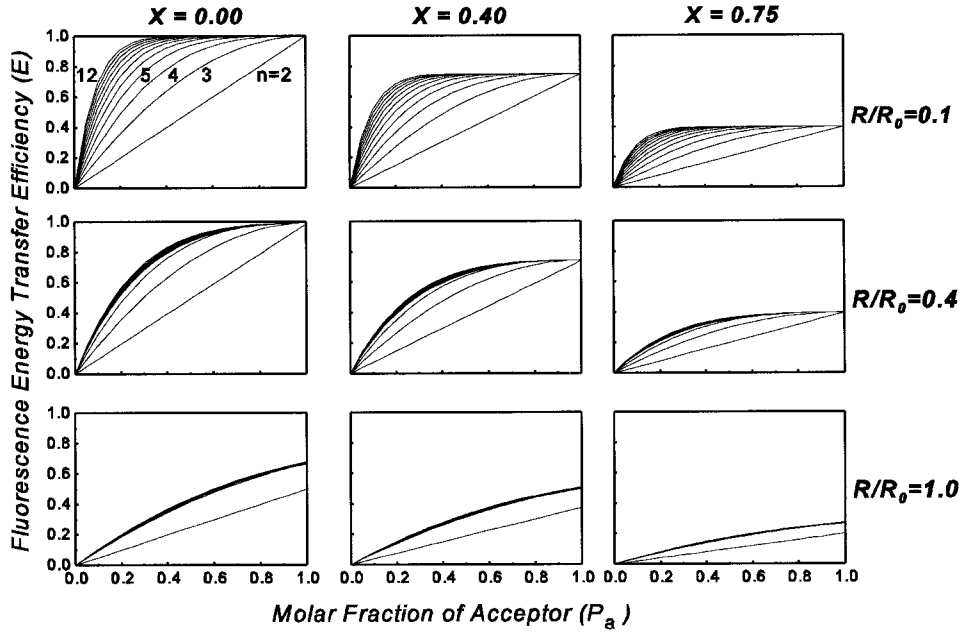

FIGURE 2 Simulations of the efficiency (E) of fluorescence energy transfer within circular ring oligomers (Fig. 2, Eqs. 8–12), as a function of the molar fraction of acceptor (P_a) at different values of n (number of subunits in oligomer), R/R_0 (where R is the inter-subunit distance and R_0 is the Förster distance), and X (molar fraction of monomers).

tant neighbors (Moens et al., 1994; Li et al., 1996). In a system with large subunits having dimensions comparable to or greater than R_0, energy transfer past the adjacent subunit can be negligible (Moens et al., 1994), justifying the second approximation. However, this is not likely to be valid for PLB, in which the lateral separation of subunits is likely to be less than R_0 (Arkin et al., 1994). The first approximation (equal energy transfer) has been useful for distinguishing dimers from higher oligomers (Veatch and Stryer, 1977; Adair and Engelman, 1994), because the dimer is the only case where E vs. P_a is linear in any model. However, this approximation does not permit the accurate analysis of large oligomers.

In the present study, we simulate the fluorescence energy transfer within oligomers that are assembled in a symmetrical ring structure (Fig. 1). For each donor-labeled subunit, energy transfer to each acceptor-labeled subunit within the oligomer is calculated explicitly, making neither of the approximations discussed above. We first calculate the time-resolved fluorescence, assuming pulsed excitation; then the steady-state fluorescence and energy transfer efficiency.

An individual subunit as a monomer, labeled with donor, will have normalized fluorescence intensity decay $F_{(t)/F(0)} = \exp(-k_D t)$. For a dimer, the second subunit will be either an acceptor (with probability P_a) or a donor (with probability $1 - P_a$), so there will be two components in the decay, $(1 - P_a)\exp(-k_D t)$ and $P_a\exp[-(k_D + k_2)t]$, where k_2 is the rate constant for energy transfer to the acceptor at position 2. Each additional subunit (indexed by j) will double the number of fluorescence decay components, adding energy transfer rate k_j with probability P_a to all previous terms, and with probability P_d ($= 1 - P_a$) adding zero to the rate of all previous terms. E.g., for a trimer, the normalized fluores-

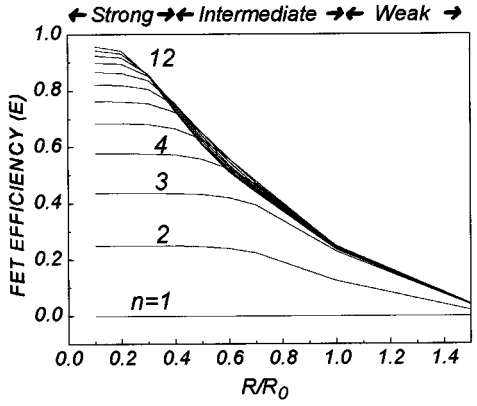

FIGURE 3 Simulations of Fig. 3, replotted to illustrate the dependence of FET on R/R_0, for the three distance ranges discussed in the text.

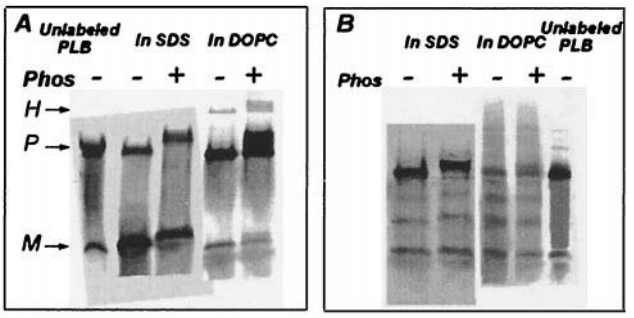

FIGURE 4 Western-blot of dye-labeled PLB after SDS-PAGE. 20 ng dye-labeled PLB in SDS solution and DOPC bilayers, run on 16.5% *tris*-tricine gel, followed by immunoblot to show the bands of dye-labeled PLB. (*A*) PLB labeled with AMCA-S and DABCYL (50% AMCA-PLB + 50% DABC-PLB); (*B*) PLB labeled with DANSCL and DABSCL (50% DANS-PLB + 50% DABS-PLB). M, monomer; P, pentamer; H, higher oligomer; Phos, phosphorylation.

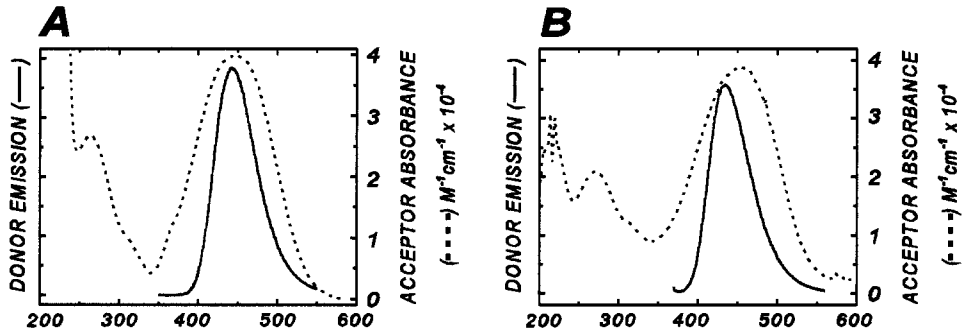

FIGURE 5 Donor fluorescence emission (- - - -) and acceptor absorbance (——) spectra measured in DOPC. (*A*) AMCA-PLB and DABC-PLB dye pair; (*B*) DANS-PLB and DABS-PLB dye pair.

cence decay would be

$$\frac{F(t)}{F(0)} = P_dP_d\exp(-k_dt) + P_aP_d\exp(-(k_D + k_2)t) + P_dP_a\exp(-(k_D + k_3)t) + P_aP_a\exp(-(k_D + k_2 + k_3)t).$$

For a given donor, note that the resulting rate constant is a sum of rate constants contributed by each acceptor, so the exponential fluorescence decay terms are multiplied, giving the general expression for the time-resolved fluorescence intensity decay,

$$\frac{F(t)}{F(0)} = \exp(-k_Dt)\prod_{j=2}^{n}[P_d + P_a\exp(-k_jt)] = \sum_{m=1}^{2^{n-1}} a_m\exp(-t/\tau_m), \quad (8)$$

where k_D is the decay rate of the donor alone, and k_j is the energy transfer rate to an acceptor on subunit j, which is given by the Förster (1948) expression,

$$k_j = k_D(r_j/R_0)^{-6}, \quad (9)$$

where r_j, the distance between the donor and the acceptor on subunit j in the n-mer ring (Fig. 1), is given by

$$r_j = 2(C_n/R_0)\sin[\pi(j-1)/n], \qquad C_n = R/[2\sin(\pi/n)]. \quad (10)$$

As illustrated in Fig. 1, C_n is the apparent radius of the n-mer, R is the distance between dye molecules on adjacent subunits ($R = r_2$), and R_0 is the Förster distance. Radius C_n is the actual radius of the n-mer only if the dye is at the center of the subunit. A model other than a ring would require a different expression for r_j. Asymmetric models would require a separate version of Eq. 10 for each unique position in the oligomer.

Labeling of subunits is assumed to be random, so the terms are independent of each other and can be multiplied as indicated in Eq. 8. Subunit 1 is the donor being considered, so the product starts at $j = 2$, resulting in 2^{n-1} exponential terms having lifetimes τ_m (Eq. 8). An algorithm was written to calculate the complete time-dependent decay of Eq. 8. As discussed below, this multi-exponential function could be analyzed directly by fitting it to time-resolved data, allowing n and R to vary until χ^2 is minimized. However, given the large number of different lifetimes (2^{n-1}) predicted by Eq. 8, for even a fairly small oligomer, it is usually more practical to calculate the steady-state fluorescence, F_{DA}, and the corresponding transfer efficiency E.

$$F_{DA} = \int_0^\infty F(t)\,dt = \left(\sum_{m=1}^{2^{n-1}} a_m\tau_m\right)\Big/\left(\sum_{m=1}^{2^{n-1}} a_m\right) = \langle\tau\rangle \quad (11)$$

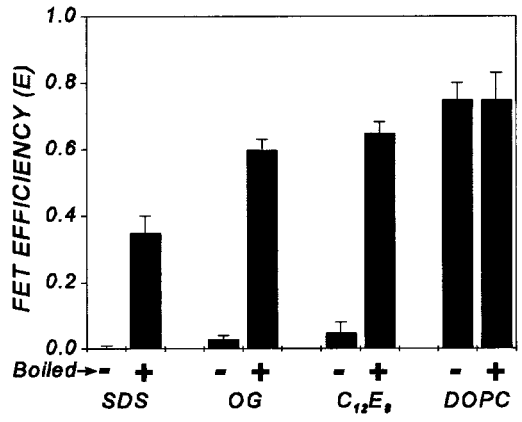

FIGURE 6 Effect of boiling on fluorescence energy transfer efficiency (E) from AMCA-PLB (donor) to DABCYL-PLB (acceptor), mixed at a ratio of 1:1 ($P_a = 0.5$). In detergents, none of the samples showed significant energy transfer before boiling (−), whereas all showed energy transfer after boiling (+). In lipid (DOPC), the boiling was done after mixing the donor and acceptor in $C_{12}E_8$, before reconstituting into DOPC. Error bars indicate SEM ($n = 3$).

TABLE 1 Effects of boiling on light scattering and fluorescence of AMCA-PLB

% change upon boiling	In SDS	In OG	In $C_{12}E_8$
Light scattering	+38 ± 8%	+300 ± 20%	+280 ± 17%
Fluorescence	−35 ± 4%	−60 ± 6%	−65 ± 5%

AMCA-PLB was mixed with DABCYL-PLB at a molar ratio of 1. Fluorescence was measured as the peak intensity in the emission spectrum. Light scattering was measured as the peak intensity at the excitation wavelength in the emission spectrum.

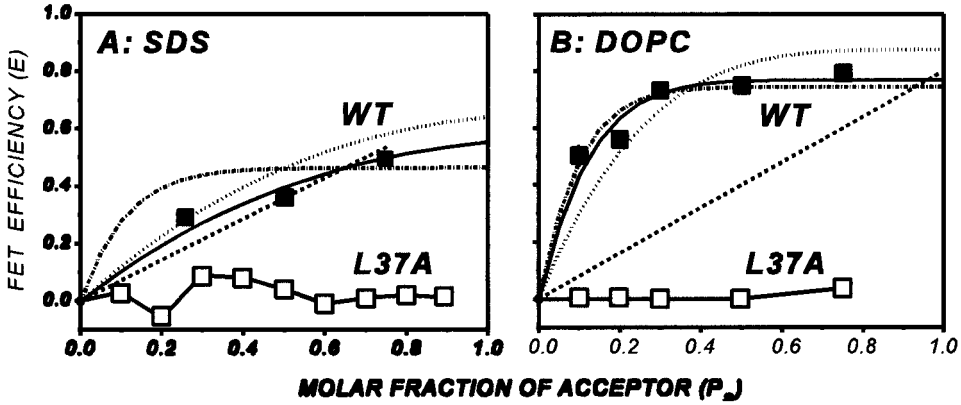

FIGURE 7 Fluorescence energy transfer of AMCA/DABCYL-PLB. (*A*) Data measured in SDS for WT-PLB (■) was best fit to $n = 5$ (——), using the simulations illustrated in Fig. 2 and Eqs. 8–12. Curves also show fits to $n = 2$ (· · · ·), $n = 8$ (- - - -) and $n = 11$ (- · - ·). (*B*) Data measured in lipid (DOPC) bilayers for WT-PLB (■) was best fit to $n = 8$ (——). Curves also show fits to $n = 2$ (· · · ·), $n = 5$ (- - - -) and $n = 11$ (- · - ·). In both SDS (*A*) and DOPC (*B*), data measured for mutant L37A-PLB (□) shows no FET, indicating that it is monomeric in both cases. Size of points indicates SEM ($n = 3$).

and

$$E = 1 - \langle\tau\rangle k_D = 1 - \langle\tau_{DA}\rangle/\langle\tau_D\rangle = 1 - F_{DA}/F_D$$

In the general case, the oligomeric structure is likely to be in equilibrium with a molar fraction X of monomers, as has been suggested by SDS-PAGE of PLB and its mutants (Wegener et al., 1984; Simmerman et al., 1996; Arkin et al., 1994; Li et al., 1998). In most cases, donors on monomeric subunits would be too far from acceptors for detectable energy transfer, so we assume that $E = 0$ for these donors. In this case, the observed (apparent) energy transfer efficiency is given by

$$E_{OBS} = (1 - X)E, \tag{12}$$

where E is given by Eq. 11. Simulations of energy transfer efficiency (E) versus molar fraction of acceptor (P_a) are plotted in Fig. 3, for various values of n, R/R_0, and X.

It is useful to discuss three regimes, which are illustrated in Fig. 3: $R/R_0 \geq 1$ (weak transfer, Fig. 2, *bottom*); $0.3 \leq R/R_0 < 1$ (intermediate transfer, Fig. 2, *middle*); $R/R_0 < 0.3$ (strong transfer, Fig. 2, *top*). In the weak transfer range (Fig. 2, *bottom row*), the inter-subunit distance R is so large that only nearest neighbors in the ring structure contribute significantly to energy transfer, so the total energy transfer E is virtually the same for trimer and up ($n \geq 3$) (Moens et al., 1994). In this range, there is maximal sensitivity to R, which can be measured unambiguously as long as $n \geq 2$ (Fig. 3). In the intermediate transfer range (Fig. 2, *middle row*), more subunits contribute to transfer, so there is moderate sensitivity to oligomeric size up to $n = 5$, and there is also moderate sensitivity to R (Fig. 3). In the strong transfer range (Fig. 2, *top row*), energy transfer efficiency to an acceptor on any subunit in the same oligomer is virtually 1, allowing the binomial expansion in Eq. 7 to be used, with $E_i(R)$ approaching 1 for all values of R. This offers increasing sensitivity to oligomeric size, but decreasing sensitivity to R. Fig. 3 facilitates the graphical estimate of errors and sensitivity, and illustrates which oligomeric states might be resolved under different conditions.

It is clear from the simulations in Fig. 2 that the monomeric fraction X can be determined independently of n and R, as long as the R is short enough to reach the intermediate or strong transfer range, so that the FET levels off at high P_a. The curvature of the plots in Fig. 2 depends on both n and R, but their effects are often distinguishable. For example, a steep slope at low P_a is only consistent with a very short value of R (*top row* of Fig. 2), and the difference between a dimer and a trimer is always clear, regardless of R.

In principle, time-resolved fluorescence can be used to obtain more detailed information about the distribution of donor/acceptor distances, and thus to remove ambiguity in data analysis. In the intermediate transfer range ($0.3 \leq R/R_0 < 1$), the number (2^{n+1}) of lifetimes τ_m (Eq. 8) is likely to be much greater than the 3 or 4 that are typically resolvable in a time-resolved fluorescence measurement, but, in the weak or strong transfer limits, the data should be much simpler. In the weak transfer range ($R/R_0 \geq 1$), only nearest neighbors affect the data, so the number of lifetimes should

TABLE 2 Fit results for FET of AMCA/DABCYL-PLB in SDS

$n =$	2	3	4	5	6	7	8	9	10	11
R (Å)	30.1	29.4	32.5	32.0	31.3	31.0	41.9	39.4	32.2	11.9
X	0.246	0.453	0.212	0.342	0.217	0.464	0.244	0.276	0.301	0.577
χ^2	4.69	**2.69**	**2.83**	**2.52**	**2.8**	**2.9**	4.87	5.87	9.83	6.26

Data in Fig. 7 *A* was fit to Eqs. 8–12. Bold numbers indicate best fits. n is the number of subunit in the oligomer. R is the inter-subunit distance within the oligomer. X is the molar fraction of protomers in monomer form.

TABLE 3 Fit results for FET of AMCA/DABC-PLB in DOPC

n =	2	3	4	5	6	7	8	9	10	11
R (Å)	21.1	17.3	4.2	12.2	12.0	15.0	8.7	10.6	12.1	13.0
X	0.000	0.000	0.118	0.125	0.175	0.212	0.219	0.230	0.231	0.231
χ^2	14.5	8.9	6.67	4.75	3.9	2.94	**2.27**	**2.1**	**2.12**	**2.02**

Data in Fig. 7 *B* was fit to Eqs. 8–12. Bold numbers indicate best fits. n is the number of subunit in the oligomer. R is the inter-subunit distance within the oligomer. X is the molar fraction of protomers in monomer form.

be three, corresponding to zero, one, or two acceptors adjacent to the donor. The distance R can be calculated directly from the second lifetime, $\tau_2 = k_D(1 \pm [R/R_0]^{-6})$ (Eqs. 9 and 10, setting $R = r_2$). In the strong transfer limit ($R/R_0 \ll 0.5$), only two lifetimes should be observed: the lifetime of the unquenched donors (donors having no acceptors in the oligomer) and a very short lifetime from donors that are strongly quenched by one or more acceptors in the oligomer.

Fitting of the experimental data

Experimental data were acquired and plotted as E vs. P_a. For each value of n (2–11), these experimental plots were fit to the theoretical curves of Fig. 2, with R and X as variables, minimizing χ^2 using a downhill simplex fitting program. Best fits for each n value are plotted below and tabulated along with χ^2 values, to illustrate the range of plausible fits.

Sample characterization

The labeling stoichiometry of dye-labeled PLB was measured by comparing dye absorbance with protein concentration, using extinction coefficients determined for dye reacted with excess *N*-acetyl-lysine-amide. For DANSCL and DABSYL, the ratio of bound dye to PLB was 1.8 ± 0.2 (SEM, $n = 5$). Reaction with isolated amino acids has shown that Lys reacts most rapidly with sulfonyl chlorides, but that Cys and Tyr also have significant reactivity. To obtain more specific labeling of Lys-3, we used succinimidylesters of AMCA and DABCYL. We tested these dyes by reacting them with *N*-acetyl-lysine carboxylamide, *N*-acetyl-tyrosine carboxylamide, and *N*-acetyl cysteine carboxylamide (Reddy et al., 1999). All three were found to be labeled by these dyes with varying rates, Lys being the fastest reacting amino acid. We found that a 60 min treatment with 10 mM DTT at 25°C completely cleaved these dyes from either the phenolic group of Tyr or the sulphhydryl group of Cys, but not from the ϵ-amino group of Lys. We used this same treatment on PLB labeled with AMCA or DABCYL succinimidylester, resulting in a final labeling ratio of 1.0–1.2 dye/PLB. We conclude that this procedure results in complete and specific labeling of Lys-3.

On SDS-PAGE, the dye-labeled PLB samples appear as a mixture of monomer and pentamer (Fig. 4), as observed previously for unlabeled PLB (Simmerman et al., 1996; Li et al., 1998). After reconstitution into DOPC bilayers, a similar pattern was observed, with the addition of a minor component whose apparent molecular weight corresponds roughly to that of an octomer (Fig. 4).

R_0 calculation

The spectra of the donor emission and acceptor absorption for the two pairs of fluorescent dyes are shown in Fig. 5. The spectral overlap was good for both pairs, and the calculated R_0 was 49 ± 1 Å for the AMCA/DABCYL pair in SDS and 48 ± 1 Å in DOPC. For the DANS/DABSYL pair, the value was 33 ± 1 Å in SDS and 32 ± 1 Å in DOPC.

FET of PLB in detergents and lipid bilayers.

In detergent solutions at 25°C, there was little or no energy transfer, even if the solutions containing donor-labeled and acceptor-labeled PLB were mixed for several hours. How-

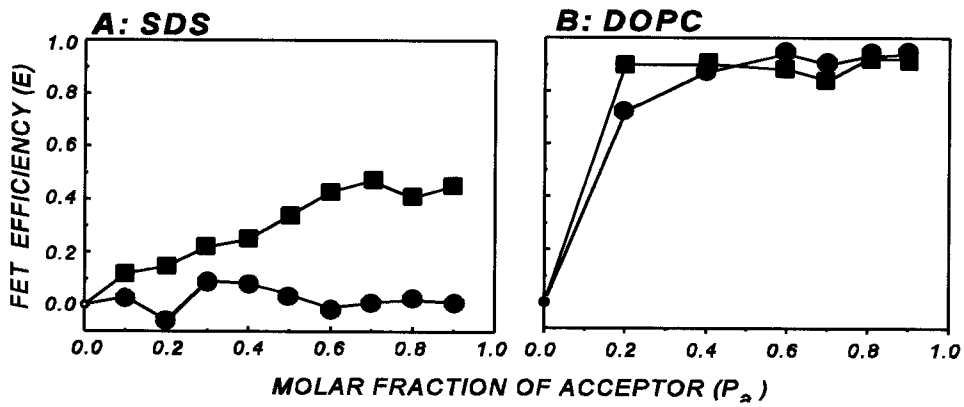

FIGURE 8 Fluorescence energy transfer of DANS/DABSYL-PLB in SDS (*A*) and DOPC (*B*). ■, sample boiled in SDS before running gel; ● not boiled.

TABLE 4 Fit results for FET of DANS/DABSYL-PLB in SDS

n =	2	3	4	5	6	7	8	9	10	11
R (Å)	25.9	20.4	28.8	28.2	30.4	27.5	26.9	27.8	26.6	26.6
X	0.242	0.516	0.393	0.409	0.312	0.427	0.435	0.411	0.443	0.443
χ^2	3.13	**1.8**	**1.9**	**1.9**	**1.94**	**1.9**	**1.9**	**1.9**	**1.86**	1.8

Data in Fig. 9 *A* was fit to Eqs. 8–12. Bold numbers indicate best fits. n is the number of subunit in the oligomer. R is the inter-subunit distance within the oligomer. X is the molar fraction of protomers in monomer form.

ever, after heating the sample to 100°C for 5 min and then cooling to 25°C for 20 min, significant energy transfer (decreased donor fluorescence in the presence of acceptor) was observed (Fig. 6, Table 1). Heating the samples for a longer time did not further decrease the fluorescence (data not shown). In all three detergents, boiling decreased fluorescence (increased energy transfer) and increased light-scattering, indicating an increase in particle size (Table 1). The increases in energy transfer and light scattering were more significant when PLB was in OG and $C_{12}E_8$ solutions, compared to that in SDS (Table 1).

In lipid (DOPC) bilayers, no boiling was required to achieve energy transfer between PLB subunits. When AMCA/DABCYL-PLB were reconstituted from detergents into DOPC bilayers, significant energy transfer (75%) occurred, whether or not the samples were boiled before mixing (Fig. 6). To ensure complete mixing of PLB subunits, samples were treated with sonication, boiling, and several freeze/thaw cycles. None of these treatments affected energy transfer efficiency, indicating that subunit mixing was complete in DOPC.

The fluorescence energy transfer efficiency E was measured for AMCA/DABCYL-PLB as a function of the molar fraction of acceptor P_a (Fig. 7). Efficiency E is higher at all P_a values in DOPC (Fig. 7 *B*) than in SDS (Fig. 7 *A*). The data in SDS (Fig. 7 *A*) fit best to $n = 3$–7, with 21–46% monomer, and an inter-subunit distance $R = 29$–32 Å (Table 2). In DOPC, the best fit was $n = 8$–11, with 22–23% monomer, and $R = 9$–13 Å (Table 3). A point mutation of PLB, in which Leu-37 is changed to Ala (L37A), results in a monomer on SDS-PAGE (Simmerman et al., 1996; Li et al., 1998). Energy transfer was negligible for L37A in both SDS and DOPC (Fig. 7, *open squares*), indicating that it is monomeric in lipid as well as in SDS.

Different FET results in detergent (SDS) and lipid (DOPC) were also seen with the DANS/DABS-PLB dye pair (Fig. 8). In SDS, there was no energy transfer when the sample was not boiled (Fig. 8 *A*). After boiling, there was significant energy transfer, and the transfer efficiency increased with the molar fraction of acceptor. In DOPC bilayers, no boiling was needed to achieve energy transfer, and much more energy transfer was observed than in SDS (Fig. 8 *B*). FET efficiency is higher in DOPC bilayers than in SDS. In SDS, analysis indicates $n = 3$–10, with 31–52% monomer, and an inter-subunit distance $R = 20$–30 Å (Fig. 9 *A*, Table 4). In DOPC, $n = 8$–11, with 7–8% monomer, and $R = 8$–10 Å (Fig. 9 *B*, Table 5).

Time-resolved fluorescence

PLB FET was investigated by time-resolved fluorescence. Acceptor-labeled PLB decreased the fluorescence lifetime of donor-labeled PLB (Fig. 10), corresponding to energy transfer from the donor to the acceptor. When FET was measured by changes in the averaged lifetimes of donor upon acceptor addition, the results were consistent with those from steady-state measurements.

The fluorescence decay was analyzed for individual lifetimes and amplitudes (Eq. 1). The lifetimes represent different fluorescent species, and the amplitudes represent their molar fractions. For AMCA/DABCYL-PLB, the fluorescence fit well to a three-exponential decay (Fig. 11). Assuming that the three lifetimes at $P_a = 0$ correspond to three conformational states of the AMCA dye on the PLB molecule, each of the three lifetime components was further fit to two subcomponents, one with the original lifetime (corresponding to no energy transfer), and one with a shorter lifetime (resulting from energy transfer to the acceptor). In this six-component fit (not shown), we found that the only new lifetimes resulting from energy transfer were very short—on the order of 0.01 ns or less, near the instrumental limit of time resolution. Therefore, we simplified the analysis to a four-component fit with the original three lifetimes fixed (Fig. 12). In this case, the shortest lifetime component corresponds to those donors that are transferring energy to acceptors, and the other three lifetime components correspond to the untransferred species that were present before the acceptor was added. The observation that the original three lifetimes ($\tau_1 = 4$ ns, $\tau_2 = 1$ ns, and $\tau_3 = 0.1$ ns) were

TABLE 5 Fit results for FET of DANS/DABSYL-PLB in DOPC

n =	2	3	4	5	6	7	8	9	10	11
R (Å)	14.2	11.6	2.8	3.5	13.0	16.0	7.8	9.9	9.7	9.6
X	3E-5	5E-5	0.118	0.035	0.197	0.131	0.079	0.070	0.071	0.070
χ^2	20	11	9.3	4.2	9.5	8.1	**1.05**	**0.98**	**0.95**	**1.0**

Data in Fig. 9 *B* was fit to Eqs. 8–12. Bold numbers indicate best fits. n is the number of subunit in the oligomer. R is the inter-subunit distance within the oligomer. X is the molar fraction of protomers in monomer form.

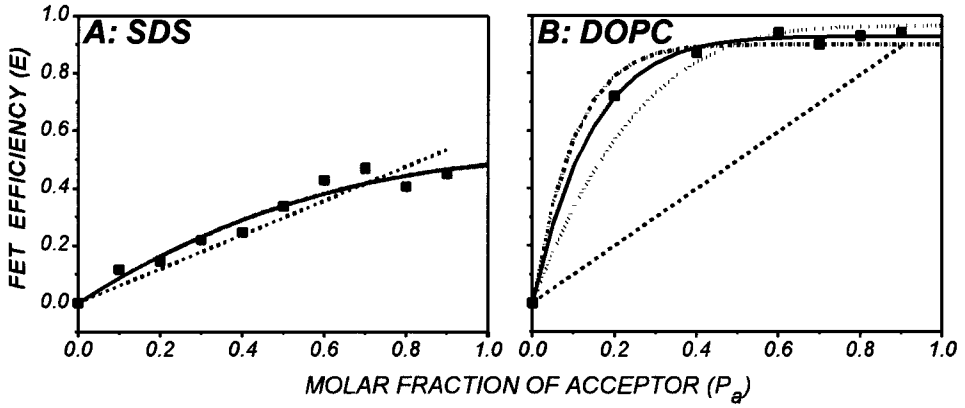

FIGURE 9 Fluorescence energy transfer of DANS/DABSYL-PLB. (*A*) Data in SDS solution (■) was best fit to $n > 3$ (——). Curve also shows fit to $n = 2$ (····). (*B*) Data in lipid (DOPC) bilayers (■) was best fit to $n = 8$ (——). Curves also shows fits to $n = 2$ (····), $n = 5$ (- - - -) and $n = 11$ (-·-·).

all quenched to one single short lifetime ($\tau_4 = 0.01$ ns) indicates that the energy transfer efficiency was very high ($E > 0.99$), corresponding to the strong transfer limit. Distance R was calculated to be <17 Å. This is consistent with the results from steady-state measurements.

When comparing the fluorescence lifetimes and amplitudes of AMCA-PLB in SDS and DOPC, we found that the difference in PLB FET in SDS and DOPC is mainly the result of differences in the amplitude (molar fraction): there is more of the shortest lifetime component (74 vs. 45%) and less of the longest lifetime component (2 vs. 23%) in DOPC than in SDS (Table 6). Because the shortest lifetime component corresponds to the active transferring species and the longest lifetime component corresponds to the untransferred species (monomer plus donor-only oligomers), we conclude that there were more monomers or donor-only oligomers when PLB was in SDS compared to that in DOPC. Assuming complete mixing and random association of PLB subunits in both SDS and DOPC, the molar fraction of donor-only oligomer should be the same in SDS and DOPC, so the 21% (23 − 2%) difference in the molar fraction of the longest lifetime in SDS and DOPC indicates that there are 21% more monomers in SDS than in DOPC. This is consistent with the steady-state results (Tables 2 and 3, 21–46% in SDS and 22–23% in DOPC).

The fluorescence lifetimes were also different in SDS and DOPC: the shortest τ was 0.08 ns in SDS and 0.01 ns in DOPC (Table 6). The corresponding R values were calculated to be 25 Å in SDS and <17 Å in DOPC. These results are consistent with those from steady-state measurements (Tables 2 and 3, 29–32 Å in SDS and 9–13 Å in DOPC). Similar results were obtained with the DANS/DABSYL-PLB fluorescence.

Effect of phosphorylation on PLB FET

The effects of PLB phosphorylation at Ser-16 on its FET in DOPC bilayers are shown in Fig. 13. Phosphorylation decreased the FET between AMCA/DABCYL-PLB, but not between DANS/DABSYL-PLB. Data analysis suggests that the decrease in FET with AMCA/DABC-PLB corresponds to a 10% increase in the monomer fraction (Table 7).

Time-resolved data shows that phosphorylation did not change the individual lifetimes, but changed the amplitudes (molar fractions): the amplitude of the longest lifetime component increased and the amplitude of the shortest lifetime component decreased (Fig. 12), suggesting that the molar fraction of monomer increased. This is consistent with the steady-state results (Table 7).

DISCUSSION

Dynamic equilibrium of PLB oligomers

Our FET method requires complete mixing and random association of the donor- and acceptor-labeled subunits in

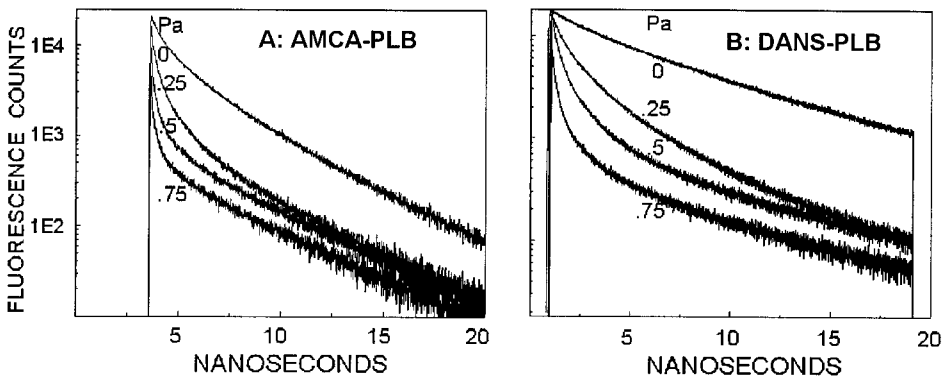

FIGURE 10 Time-resolved fluorescence of donor-PLB in DOPC bilayers. Numbers stand for the molar fraction of acceptor (P_a). (*A*) AMCA-PLB; (*B*) DANS-PLB.

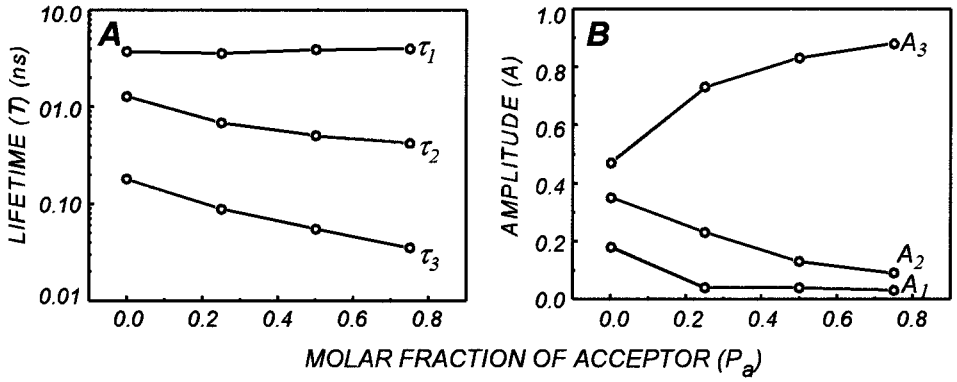

FIGURE 11 Fluorescence lifetimes (τ) and amplitudes (A) from three-exponential fit of AMCA-PLB fluorescence in DOPC. The fluorescence (Fig. 10 *A*) was fit to Eq. 1 with $n = 3$.

the sample preparation. In detergent solution, no FET was detected for PLB if it was not boiled before the measurement (Fig. 6). This is probably because heating accelerates the dissociation of PLB oligomers into monomers and the exchange of PLB molecules between detergent-protein complexes, so that the mixture of monomers can reassociate randomly into oligomers, as required. The correlation between changes in fluorescence and light scattering upon sample boiling (Table 1) suggests that aggregation of protein-detergent complexes (indicated by increase in light scattering) promotes PLB subunit mixing. After boiling the samples, both FET and light scattering were greater in OG and $C_{12}E_8$ compared to that in SDS (Table 1), perhaps because nonionic detergents (OG, $C_{12}E_8$) are more subject to aggregation upon temperature increase (cloud point) than are ionic detergents (SDS) (Schick, 1967). Further boiling of the sample, beyond the standard 5-min period, did not increase FET, which suggests that subunit mixing was complete. The observation that energy transfer is readily detected without boiling of the sample when PLB is in lipid bilayers, suggests that PLB molecules are in a dynamic equilibrium in DOPC bilayers, facilitating subunit mixing and association.

Error and sensitivity of the method: application to PLB structural measurement

The fitting results present a range of parameter values for n, R, and X. For AMCA/DABCYL-PLB pair, the SDS data (Fig. 7 *A*) fit to $n = 3$–7, with 21–46% monomer, and an inter-subunit distance $R = 29$–32 Å (Table 2). The DOPC data fit to $n = 8$–11, with 22–23% monomer, and $R = 9$–13 Å (Table 3). We have plotted this range of fits (Figs. 7 and 13) to illustrate the uncertainties. Simulations showed that the sensitivity of FET to n increases when R decreases (Fig. 3). This explains the narrower range of values for n in DOPC (8–11) compared to that in SDS (3–10) because R is smaller in DOPC than in SDS (Tables 2 and 3). From the simulation in Fig. 3, we also see that the sensitivity of FET to n diminishes while n increases, so it is difficult to extract an accurate value for n beyond 8, even under favorable conditions of R. Nevertheless, it is clear that n is greater in DOPC (8–11) than in SDS (3–7). This is consistent with the results from SDS-PAGE, in which PLB exhibits more clearly a species of higher oligomer ($n = 8$) after reconstitution into DOPC (Fig. 7). Our results suggest that PLB oligomers exist in DOPC that are much larger than the pentamers observed in SDS-PAGE. If PLB is primarily pentameric, as suggested by SDS-PAGE, then PLB pentamers themselves must be substantially aggregated in DOPC under the conditions of our measurements. To clarify this issue, further experiments will be needed in which the lipid composition and content are varied.

Time-resolved fluorescence data supports the interpretation of steady-state data

Time-resolved fluorescence was used to resolve individual lifetime components that correspond to energy transfer species. Theoretically, the donor fluorescence decay might be expected to be monoexponential in the absence of acceptor ($P_a = 0$). However, our results show that the donor fluorescence for both donor/acceptor pairs is multiexponential in the absence of acceptor (Fig. 10), suggesting that the donor experiences multiple environmental states. Despite this complication, the addition of acceptor has a strikingly

TABLE 6 Time-resolved fluorescence of AMCA/DABCYL-PLB

	P_a	τ_1 (ns)	a_1	τ_2 (ns)	a_2	τ_3 (ns)	a_3	τ_4 (ns)	a_4	χ^2
In SDS	0	4.32	0.44	1.54	0.26	0.22	0.30			1.60
	0.5	4.13	0.23	1.64	0.14	0.31	0.18	0.08	0.45	1.10
In DOPC	0	3.96	0.18	1.28	0.35	0.18	0.47			1.73
	0.5	4.04	0.02	0.81	0.04	0.14	0.20	0.01	0.74	1.08

Fluorescence was fit to Eq. 1 with $n = 4$. P_a is the molar fraction of acceptor.

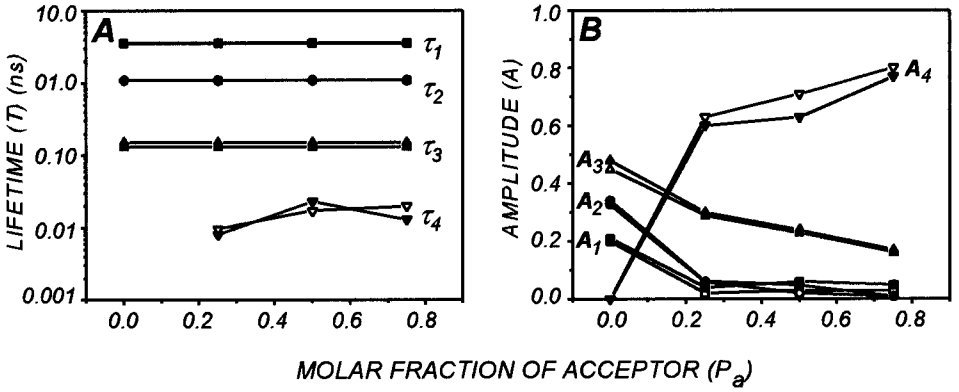

FIGURE 12 Fluorescence lifetimes (τ) and amplitudes (A) from four-exponential fit of AMCA-PLB fluorescence in DOPC. The fluorescence (Fig. 10 *A*) was fit to Eq. 1 with $n = 4$.

simple effect—the addition of a single very short lifetime ($\tau < 0.1$ ns) (Fig. 12 and Table 7). This short lifetime is not due to an increase in light scattering, because steady-state light scattering did not increase with acceptor content. Of course, such a short lifetime cannot really be measured accurately, so we can only estimate an upper bound for the distance R. Nevertheless, it is clear that the only significant change observed with increasing acceptor is the increase of the amplitude of this strongly quenched component at the expense of the other amplitudes (Fig. 12 and Table 7). As discussed in Results, this is precisely the behavior expected in the strong transfer limit, in which the distance between dyes on adjacent subunits is so short ($R \ll R_0$) that any donor in an oligomer having one or more acceptors gives rise to an extremely short lifetime that approaches the limit of instrumental resolution. The estimated value of this lifetime is thus an upper bound, yielding a transfer efficiency of >99% and a corresponding donor/acceptor distance of <17 Å. This is consistent with the results from steady-state data ($R = 9$–13 Å, Tables 3 and 4).

Time-resolved fluorescence also allowed us to resolve changes in oligomer shape (inter-subunit distance) from changes in size distribution (molar fraction of monomer). For example, analysis of the time-resolved data for AMCA/DABCYL-PLB in SDS and DOPC shows that the limiting amplitude (molar fraction) of the shortest lifetime component was 45% in SDS and 74% in DOPC (Table 6) (i.e., most of the donor-labeled PLB subunits are quenched by acceptors in DOPC, but fewer than half are quenched in SDS). This indicates clearly that there are fewer monomers or donor-only oligomers in DOPC than in SDS. In addition, the lifetime of the strongly quenched component was substantially smaller in DOPC than in SDS, suggesting a smaller distance between dyes on adjacent subunits. Thus, the time-resolved data provide direct support for the conclusions obtained from steady-state analysis data (Tables 2 and 3). These different results in detergent and lipid underscore the importance of analyzing PLB structure in its native membrane environment, even though the study of detergent solutions is more convenient.

Steady-state and time-resolved data are also consistent in the effect of PLB phosphorylation on AMCA/DABCYL-PLB FET: phosphorylation increased the monomer fraction by 10% from both measurements (Fig. 13 and Table 7).

Possible perturbation of PLB structure by fluorescent dyes—revealed by the difference in FET measured by two dye pairs

Two pairs of fluorescent dyes were used in this study. The results are similar, yet not quite the same, as illustrated in Table 8. The most significant difference is in the value of X (molar fraction of monomer) in DOPC. The number is 0.22–0.23 measured with the AMCA/DABCYL dye pair, and 0.07–0.08 with the DANS/DABSYL dye pair (Table 8). The difference in the result measured by AMCA/DABCYL and DANS/DABS dye pairs is also shown in the effects of phosphorylation. A slight decrease in FET upon PLB phosphorylation was detected with the AMCA/

TABLE 7 Fit results for FET of AMCA/DABCYL-PLB, effect of phosphorylation

		n									
	phos	2	3	4	5	6	7	8	9	10	11
R (Å)	−	21	17	4	8	16	13	14	15	15	16
	+	22	20	27	6	24	16	25	17	21	16
X	−	0	0	0.12	0.13	0.17	0.18	0.18	0.18	0.18	0.22
	+	0	0.17	0.21	0.30	0.24	0.33	0.25	0.33	0.27	0.33
χ^2	−	16	8.5	5.8	3.3	2.4	**1.2**	**1.2**	**1.2**	**1.2**	2.7
	+	4.7	3.1	2.5	2.1	2.1	**1.9**	**2.1**	**1.9**	**2**	**1.7**

Data in Fig. 13 *A* was fit to Eqs. 8–12. Bold numbers indicate best fits. n is the number of subunit in the oligomer. R is the inter-subunit distance within the oligomer. X is the molar fraction of protomers in monomer form.

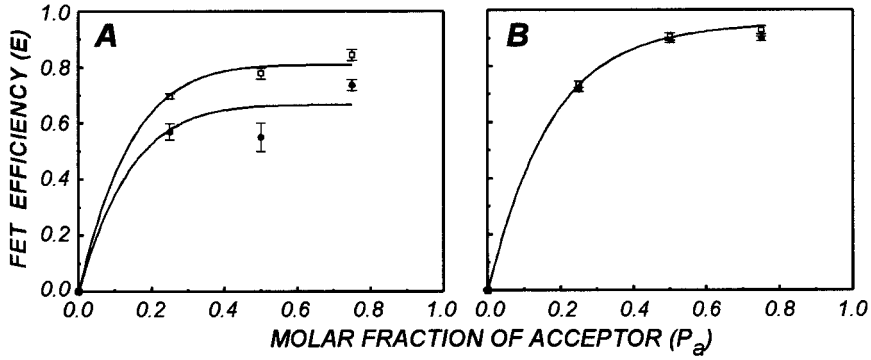

FIGURE 13 Effect of phosphorylation on PLB fluorescence energy transfer. (*A*) FET measured with AMCA/DABC-PLB. Curves correspond to best fit for unphosphorylated PLB. □, with $n = 8 \pm 2$, $X = 18 \pm 0\%$, $R = 14 \pm 1$ Å, for phosphorylated PLB; ●, with $n = 8 \pm 2$, $X = 27 \pm 6\%$, $R = 17 \pm 8$ Å. (*B*) FET measured with DANS/DABS-PLB. Curves correspond to best fit for both unphosphorylated (□) and phosphorylated PLB. ●, with $n = 8$–11, $X = 8 \pm 1\%$ and $R = 10 \pm 2$ Å.

DABCYL dye pair, but no change was seen with the DANS/DABSYL pair (Fig. 13). This difference suggests a structural perturbation of PLB by dye labeling. The lower monomeric fraction observed with DANS might be the result of aggregation caused by the DANS moiety, which is more hydrophobic than AMCA. The most obvious effect of phosphorylation is to change the charge of PLB, so the difference in the phosphorylation response between these two dye pairs could be because of their difference in charge, as discussed below.

Relationship to other work

Our results clearly show that wild-type PLB is oligomeric in both SDS solution (consistent with SDS-PAGE, Fig. 4) and in lipid bilayers, whereas the point mutant L37A-PLB remains monomeric under both sets of conditions. These results are consistent with a previous EPR study (Cornea et. al, 1997), but our results reveal much more than the EPR method, which does not have the resolution to distinguish a change in the monomeric fraction from a change in the size of the oligomeric fraction. Our result shows clearly that PLB exists as a mixture of oligomer and monomer, with the molar fraction of monomer being 7–23% in DOPC. The steady-state FET method (Fig. 2) can clearly resolve monomers from oligomers, but it probably lacks the sensitivity to reveal a more complex distribution of oligomeric sizes. It is likely that more extensive use of the time-resolved method (Fig. 10) will be needed to make progress in that direction.

Our phosphorylation results show a slight decrease in oligomerization with one dye pair and no change with the other, in apparent disagreement with the EPR study, which showed a slight increase in PLB oligomerization upon phosphorylation (Cornea et. al, 1997). The most likely explanation for the different phosphorylation effects for these three cases is that the different probes result in different electrostatic charges on PLB. In the EPR study, lipid spin labels were used, so PLB was unmodified. Phosphorylation changes the net charge on PLB's cytoplasmic domain (residues 1–24) from +2 to 0, which should decrease electrostatic repulsion and promote oligomerization, as observed by EPR (Cornea et al., 1997). Reaction of Lys-3 with AMCA-S (net charge −1) changes the net charge on the cytoplasmic domain from +2 to 0, and phosphorylation changes this charge from 0 to −2, which should increase electrostatic repulsion and decrease oligomerization, as observed in the present study. Reaction with DANSCL (net charge 0) produces a net charge of +1, and phosphorylation changes this charge to −1, which should cause no change in electrostatic repulsion or aggregation state of PLB, as observed. This analysis suggests that the EPR result (Cornea et al., 1997), indicating increased oligomerization of PLB by phosphorylation, is most likely to be representative of unmodified PLB, and that electrostatic interactions play a central role in the oligomeric state of PLB.

It has been predicted that the function of PLB, regulation of the Ca-ATPase, depends critically on its oligomeric state (Cornea et al., 1997; Simmerman et al., 1996). Testing this hypothesis will require measurement of the oligomeric state of PLB in the presence of the Ca-ATPase as a function of PLB phosphorylation. This is not feasible with the previously used EPR method (Cornea et al., 1997), because that method relied on lipid spin labels to measure the surface area of all proteins in the membrane, without specificity for PLB. It is feasible with the present method, which involves the specific labeling of PLB. This method has been successfully applied to study PLB oligomeric structure in the presence of Ca-ATPase, showing that the Ca-ATPase increases the monomeric fraction of PLB (Reddy et al., 1999).

TABLE 8 Comparison of the results measured with two dye pairs

	in SDS			in DOPC		
Dye pair	*n*	*R* (Å)	*X*	*n*	*R* (Å)	*X*
AMCA/DABCYL	3–7	29–32	0.21–0.46	8–11	9–13	0.22–0.23
DANS/DABSYL	3–10	20–30	0.31–0.52	8–11	8–10	0.07–0.08

n is the number of subunits in the oligomer, *R* is the inter-subunit distance within oligomer, and *X* is the molar percent of protomers in monomer form.

CONCLUSIONS

We have developed a fluorescence energy transfer method, and corresponding mathematical analysis, that provides detailed insight into protein oligomeric structure. Experiments on PLB indicate that it is primarily oligomeric in both SDS solution and lipid (DOPC) bilayers, with a significant monomeric fraction in both cases. However, the extent of oligomerization, the oligomeric size, and the proximity of adjacent subunits are different in these two cases. In lipid bilayers, but not in detergent solution, there is a dynamic equilibrium between monomers and oligomers. The perturbation of this equilibrium by phosphorylation is consistent with a model in which changes in electrostatic interactions are dominant. Fluorescence energy transfer is very effective in analyzing the oligomeric structure of PLB, and the experimental and analytical methods developed here should be applicable to a wide range of other oligomeric proteins, in membranes or in solution.

We thank Frank Prendergast for making the time-resolved fluorescence facilities available and Eric Olson and Dehong Hu for help with the time-resolved fluorescence measurement.

REFERENCES

Adair, B. D., and D. M. Engelman. 1994. Glycophorin a helical transmembrane domains dimerize in phospholipid bilayers: a resonance energy transfer study. *Biochemistry.* 33:5539–5544.

Arkin, I. T., P. D. Adams, K. R. MacKenzie, M. A. Lemmon, A. T. Brunger, and D. M. Engelman. 1994. Structure organization of the pentameric transmembrane α-helices of phospholamban, a cardiac ion channel. *EMBO J.* 13:4757–4764.

Autry, J. M., and L. R. Jones. 1997. Functional co-expression of the canine cardiac Ca^{2+}-pump and phospholamban in Sf21 cells reveals new insights on ATPase regulation. *J. Biol. Chem.* 272:15872–15880.

Chen, R. F. 1966. Fluorescence quantum yield of 1-dimethylaminonaphthalene-5-sulphonate. *Nature.* 209:69.

Cornea, R. L., L. R. Jones, J. M. Autry, and D. D. Thomas. 1997. Mutation and phosphorylation change the oligomeric state of phospholamban in lipid bilayers. *Biochemistry.* 36:2960–2967.

Colyer, J. 1993. Control of the calcium pump of cardiac sarcoplasmic reticulum. A specific role for the pentameric structure of phospholamban? *Cardiovasc. Res.* 27:1766–1771.

Förster, T. 1948. Intermolecular energy migration and fluorescence. *Ann. Phys.* 2:55–75.

Kimura, Y., K. Kurzydlowski, M. Tada, and D. H. MacLennan. 1997. Phospholamban inhibitory function is activated by depolymerization. *J. Biol. Chem.* 272:15061–15064

Kovacs, R. J., M. T. Nelson, H. K. Simmerman, and L. R. Jones. 1988. Phospholamban forms Ca^{2+}-selective channels in lipid bilayers. *J. Biol. Chem.* 263:18364–18368.

Li, M., R. L. Cornea, E. J. Olson, L. R. Jones, and D. D. Thomas. 1996. The oligomeric structure of phospholamban in membranes probed by fluorescence energy transfer. *Biophys. J* 70:A284.

Li, M., L. R. Jones, R. L. Cornea, and D. D. Thomas. 1998. Phosphorylation-induced structural change in phospholamban and its mutants, detected by intrinsic fluorescence. *Biochemistry.* 37:7869–7877.

Lindemann, J. P., L. R. Jones, D. R. Hathaway, B. G. Henry, and A. M. Watanabe. 1983. β-adrenergic stimulation of phospholamban phosphorylation and Ca^{2+}-ATPase activity in guinea ventricles. *J. Biol. Chem.* 258:464–471.

Luo, W., I. L. Grupp, J. Harrer, S. Ponniah, G. Grupp, J. J. Duffy, T. Doetschman, and E. G. Kranias. 1994. Targeted ablation of the phospholamban gene is associated with markedly enhanced myocardial contractility and loss of β-agonist stimulation. *Circ. Res.* 75:401–409.

Moens, P. D., D. J. Yee, and C. G. dos Remedios. 1994. Determination of the radial coordinate of Cys-374 in F-actin using fluorescence resonance energy transfer spectroscopy: effect of phalloidin on polymer assembly. *Biochemistry.* 33:13102–13108.

Reddy, L. G., L. R. Jones, and D. D. Thomas. 1999. Depolymerization of phospholamban in the presence of calcium pump: a fluorescence energy transfer study. *Biochemistry*. In press.

Reddy, L. G., R. C. Pace, L. R. Jones, and D. L. Stokes. 1995. Functional reconstitution of recombinant phospholamban with rabbit skeletal Ca^{2+}ATPase. *J. Biol. Chem.* 270:9390–9397.

Schaffner, W., and C. Weissman. 1973. A rapid, sensitive, and specific method for the determination of protein in dilute solutions. *Anal. Biochem.* 56:502–514.

Schick, M. J. 1967. Nonionic Surfactants. Marcel Dekker, Inc., New York.

Simmerman, H. K. B., and L. R. Jones. 1998. Phospholamban: protein structure, mechanism of action, and role in cardiac function. *Physiol. Rev.* 78:921–947.

Simmerman, H. K. B., Y. M. Kobayashi, J. M. Autry, and L. R. Jones. 1996. A leucine zipper stabilizes the pentameric membrane domain of phospholamban and forms a coiled-coil pore structure. *J. Biol. Chem.* 271:5941–5946.

Vanderkooi, J. M., A. Lerokomar, H. Nakamura, and A. Martinosi. 1977. Fluorescence energy transfer between Ca transport ATPase molecules in artificial membranes. *Biochemistry.* 16:1262–1267.

Veatch, W., and L. Stryer. 1977. The dimeric nature of the gramicidin A transmembrane channel: conductance and fluorescence energy transfer studies of hybrid channels. *J. Mol. Biol.* 113:89–102

Watanabe, Y., Y. Kijima, M. Kadoma, M. Tada, and T. Takagi. 1991. Molar weight determination of phospholamban oligomer in the presence of sodium dodecyl sulfate: application of low-angle laser light scattering photometry. *J. Biochem.* 110:40–45.

Wegener, A. D., and L. R. Jones. 1984. Phosphorylation-induced mobility shift in phospholamban in sodium dodecyl sulfate-polyacrylamide gels. *J. Biol. Chem.* 259:1834–1841.

Wegener, A. D., H. K. B. Simmerman, J. P. Lindemann, and L. R. Jones. 1989. Phospholamban phosphorylation in intact ventricles. *J. Biol. Chem.* 264:11468–11474.